Petroleum Science 19 (2022) 2374–2386

Contents lists available at ScienceDirect

Petroleum Science

journal homepage: www.keaipublishing.com/en/journals/petroleum-science

Original Paper

Experimental investigation on migration and retention mechanisms of elastic gel particles (EGPs) in pore-throats using multidimensional visualized models

Yi-Fei Liu [a, b], Chen-Wei Zou [a, b], Xu-Guang Lou [c], Ming-Wei Gao [a, b], Guang Zhao [a, b], Ming-Wei Zhao [a, b, *], Cai-Li Dai [a, b, **]

[a] Shandong Key Laboratory of Oilfield Chemistry (China University of Petroleum (East China)), Qingdao, 266580, PR China
[b] Key Laboratory of Unconventional Oil & Gas Development (China University of Petroleum (East China)), Ministry of Education, Qingdao, 266580, PR China
[c] China Southern Petroleum Exploration & Development Corporation, Haikou, Hainan, 570216, People's Republic of China

ARTICLE INFO

Article history:
Received 9 January 2022
Received in revised form
16 May 2022
Accepted 17 May 2022
Available online 26 May 2022

Edited by Xiu-Qiu Peng

Keywords:
Enhanced oil recovery
Elastic gel particles
Matching coefficient
In-depth profile control
Pore-throat visualization models

ABSTRACT

Knowledge of migration and retention mechanisms of elastic gel particles (EGPs) in pore-throats is essential for the effective application of EGPs as a smart sweep improvement and profile control agent for enhanced oil recovery (EOR). The matching coefficient (defined as the ratio of particle size to pore-throat size) is used to investigate its influence on migration, retention and profile control performance of EGPs. A 1-D continuous pore-throat visualization model (PTVM), a 2-D heterogeneous PTVM and a 3-D heterogeneous core model were constructed and used to investigate pore-scale migration, retention and controlling mechanism of migration and retention characteristics on EGPs profile control. The results of the 1-D continuous PTVM indicated that while the matching coefficient was in the optimal range (i.e., 0.20–0.32), the EGPs could not only smoothly migrate to the deeper pore-throats, but also form stable retention in the pores to resist the erosion of injected water, which was conducive to the effective in-depth profile control. The results of the 2-D heterogeneous PTVM verified that the sweep efficiency in low-permeability regions could be significantly improved by in-depth migration and stable retention of EGPs in the pore-throats with an optimal matching coefficient (0.29), which was much better than that in cases with a smaller matching coefficient (0.17) or an excessive matching coefficient (0.39). Moreover, the NMR displacement experiments of 3-D heterogeneous cores were carried out to simulate the EGPs profile control in actual reservoir porous media. Saturation images and T_2 spectrum curves of crude oil showed that EOR in the low-permeability layer was highest (56.1%) using EGPs profile control with an optimal matching coefficient, attributing to the in-depth migration and stable retention of EGPs.

1. Introduction

Water injection has been extensively applied in oilfields for enhanced oil recovery (EOR) because of its low cost and easy operation (You et al., 2019; Zhou et al., 2020; Wang et al., 2021). However, almost all reservoirs are heterogeneous, which means that there are oil layers with different permeabilities in the reservoir or dominant channels exist in the same oil layer. With continuous erosion by injected water, the heterogeneity of a reservoir can become more severe (Goudarzi et al., 2013; Liu, 1995). The serious heterogeneity of reservoirs results in the invalid displacement of injected water along the high permeability layers or the dominant channels, and hence oil-bearing areas with low permeability can remain unswept (Bai et al., 2007). This leads to low efficiency water injection, high purification costs of production water and higher potential environmental pressures. It has been estimated that about 70% of the crude oil underground in typical

* Corresponding author. School of Petroleum Engineering, China University of Petroleum (East China), No. 66, West Changjiang Road, Huangdao District, Qingdao, 266580, China.
** Corresponding author. School of Petroleum Engineering, China University of Petroleum (East China), No. 66, West Changjiang Road, Huangdao District, Qingdao, 266580, China.
E-mail addresses: zhaomingwei@upc.edu.cn (M.-W. Zhao), daicl@upc.edu.cn (C.-L. Dai).

https://doi.org/10.1016/j.petsci.2022.05.010

oil-bearing geology cannot be displaced out due to the poor sweep efficiency of water injection (Liu et al., 2010; Sang et al., 2014).

Profile control is a widely applied technique used to expand the swept volume of injected water to improve oil recovery (Liu et al., 2010). By blocking water channels, the subsequent injected water is diverted to the previously unswept low permeability zones with high remaining oil saturation. Injection of chemical profile control agents, such as polymers, cross-linked polymer gels, foams, elastic gel particles, etc., is widely applied in oilfields for profile control treatment (Kabir, 2001; Wang et al., 2008; Liu et al., 2016, 2017; Zhang and Seright, 2007). Injection of elastic gel particles (EGPs), such as preformed particle gel (PPG), polyacrylamide microsphere (PEM) and dispersed particle gel (DPG), is a cutting-edge technique for profile control (Wu and Bai, 2008; Liu et al., 2016; Long et al., 2018; Tang et al., 2018). The EGPs profile control agent has drawn great attention in recent years due to its excellent properties, such as controllable particle sizes, a wide range of particle sizes (nanometer to millimeter), controllable particle strength, excellent shear resistance and easy injection for in-depth profile control (Feng et al., 2020; You et al., 2014; Elsharafi and Bai, 2017).

An EGP-based system is a discontinuous phase, and the migration and retention of particles in porous media of reservoirs is complex (Yao et al., 2014; Zhu et al., 2021; Lei et al., 2021; Cui et al., 2021). The retention and migration behaviors of particles have extreme impact on the profile control effect of an EGP-based system (Yao et al., 2014; Zhu et al., 2021; Lei et al., 2021). The elasticity of the particles enables them to pass through pore-throats within the porous media under the injection pressure, representing migration of particles. They can also be captured by pore-throats, representing retention. However, if most particles migrate through the pore-throats and cannot form sufficient retention in the pores, the profile control capability of the EGPs system will be weak. Therefore, the balance between migration and retention is conducive to the in-depth profile control performance of the EGPs system. The necessary condition for the EGPs system to achieve effective in-depth profile control is that the particles can both migrate through, and form a certain amount of retention in pore-throats (Zhao and Bai, 2022).

The shape and strength of particles, especially the ratio of particle size to pore-throat size, determine the migration and retention behavior of particles in porous reservoir media (Dai et al., 2017; Ren et al., 2016). Although some researchers have studied the injection and plugging properties of EGPs in porous media, and the matching relationships between particle properties and porous media properties, few studies have visualized pore-scale migration and retention mechanisms of particles. Imqam et al. (2015, 2017) designed tubes with different inner diameters to simulate the dominant channels in a reservoir and using these they investigated the impact of particle strength, the ratio of particle size to opening diameter and the injection rate on the injectivity and plugging efficiency of PPG. Using their experimental data, they developed two empirical equations to quantitatively predict the resistance factor and the stable injection pressure as functions of the above three factors. Yao et al. (2012, 2015) studied the compatibility of pore-scale elastic PEM as a profile control agent using sand-pack models. They introduced a matching factor between particle size and pore-throat diameter of the sand-pack model to characterize their matching relationship between the PEM and the porous media. The results indicated that the optimal matching factor lay within the range 1.35–1.55. Yang et al. (2017) investigated the matching mechanism between PEM with different storage modulus and porous media using a long sand-pack model. They concluded that there were five passing through patterns, and established a comprehensive correlation equation linking matching factors to passing through patterns for different storage modulus. Dai et al. (2017, 2018) studied the matching relationship between particle size of DPG and permeability of porous media using a series of core flooding experiments. They optimized the matching factor depending on both the injection pressure of DPG and the plugging rate to porous media, and their results showed that the optimal range of the matching factor was between 0.21 and 0.29.

The former studies on the migration and retention of EGPs in reservoir pore-throats exist certain deficiencies. Firstly, experimental models such as conduit models are too ideal to simulate actual reservoir porous media (Imqam et al., 2015, 2017). Secondly, most studies were carried out using non-visual models, such as the sand-pack model (Yao et al., 2012, 2015; Yang et al., 2017; Dai et al., 2017, 2018). Although the injection pressure curves during the flooding process can indirectly reflect the migration and retention law of particles, the data obtained by this method exhibits deviations and hysteresis, which cannot be accurately analyzed. In addition, the retention and migration behavior of the particles is invisible, resulting in some important processes and information being hidden.

In this work, a one-dimensional continuous pore-throat visualization model (PTVM), a two-dimensional heterogeneous PTVM and a three-dimensional heterogeneous core model were developed in order to avoid the deficiencies of simple idealized models and sand-pack models. The migration and retention characteristics of EGPs in pore-throats were visually analyzed using a one-dimensional continuous pore-throat model and the matching relationship between the particles and the pore-throats was optimized based on the migration and retention results. Using displacement experiments with the two-dimensional heterogeneous pore-throat model, the influence of the matching relationship on the in-depth profile control of EGPs was visually analyzed. Finally, using a nuclear magnetic resonance (NMR) displacement experiment with the three-dimensional heterogeneous core model, which could simulate the actual porous medium of a reservoir, the influence of migration and retention of EGPs on oil recovery from different sized pores were analyzed. The aim of this work was to elucidate the migration and retention characteristics of EGPs in pore-throats, to identify the mechanisms of migration and retention and to examine their influence on EOR using profile control by EGPs.

2. Experimental section

2.1. Materials

Non-ionic polyacrylamide (PAM) with a weight-average molecular weight of 1.0×10^7 g/mol, and polyethylene imine (PEI) as the crosslinking agent, were provided by Anjarl Oilfield Technical Services Co., Ltd., China. Crude oil and formation brine were collected from the Changqing Oilfield (Shanxi, China). The viscosity of the crude oil was 3.13 mPa s at 90°C and its density was 818 kg/m^3. The density of the formation brine was 1020 kg/m^3, and the results of an analysis of the main ion components are provided in Table 1.

Table 1
Main ion content and salinity of the formation brine collected from the Changqing oilfield.

Ions	Na^+ and K^+	Ca^{2+} and Mg^{2+}	SO_4^{2-}	Cl^-
Concentration, mg/L	2101.1	599.73	258.31	3966.79
Total salinity, mg/L	6925.93			

2.2. Methods

2.2.1. Preparation of EGPs

The EGPs was prepared using a high-speed shearing method with a colloid mill from bulk gel. The detailed procedure was reported by Liu et al. (2016). Briefly, the first step was preparation of the bulk gel. Next, a mixture of bulk gel and brine was placed into the colloid mill, then the EGPs suspension was obtained by high-speed shearing using the mill. During the preparation process, the size distribution of the EGPs could be controlled by adjusting the shearing time and rotation rate of the mill. In this work, a PEI crosslinked PAM gel was chosen as the bulk gel because of its excellent temperature resistance, salinity tolerance and environmental-friendly characteristics (Jia et al., 2010). The bulk gel was prepared with 0.4 wt% PAM and 0.6 wt% PEI at 90°C for 12 h.

2.2.2. Visual characterization of migration and retention behaviors of EGPs in pore-throats

In order to observe the migration and retention behaviors of EGPs in pore-throats directly and accurately, a one-dimensional continuous PTVM was designed and manufactured. Polymethyl methacrylate (PMMA) was used to prepare the model because of its simple manufacture and high transmittance (Wu et al., 2017). A micromodel was fabricated on a plate of PMMA by precise milling and then sealing with another PMMA plate. A schematic diagram of the one-dimensional continuous PTVM (main view and top view) is displayed in Fig. 1. The micromodel consisted of 21 identical pore-throat structures. The geometric parameters of the pores applied in this work were 1000 μm in length, 300 μm in length and 300 μm in height, and the geometric parameters of the throats were 500 μm in length, 100 μm in length and 100 μm in height.

Fig. 2 presents a schematic of the experimental setup. The inlet for the EGPs dispersion or brine water was connected to a syringe (10 mL, Hamilton, Germany) driven by syringe pumps (Harvard Apparatus, PHD2000, USA). The micromodel was placed under an inverted microscope (Leica, DM i8, Germany), which was equipped with a high-speed camera of up to 200,000 frames per second (Photron, SA-Z, Japan). In the process of EGPs injection and water flooding, the migration and retention of particles at different pore-throat positions were recorded by the camera.

The migration and retention of EGPs in pore-throats under different matching degrees were systematically assessed as the matching relationship between particles and pore-throats is a key factor affecting the migration and retention behaviors of EGPs in the porous media of a reservoir. The matching coefficient (φ) is defined as:

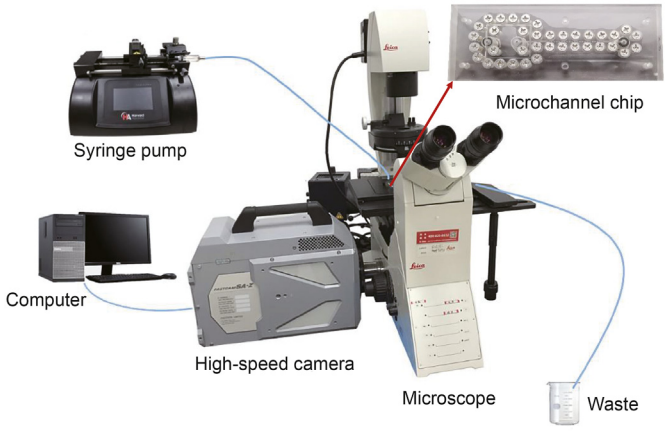

Fig. 2. Experimental setup for the one-dimensional continuous PTVM flooding.

$$\varphi = \frac{d_{\text{particle}}}{d_{\text{pore-throat}}} \tag{1}$$

where φ is the matching coefficient; d_{particle} is the average size of EGPs, μm; and $d_{\text{pore-throat}}$ is the mean diameter of pore-throats of the micromodel, μm.

The average particle diameter was measured using a laser particle size analyzer (Bettersize2000; Bettersize instruments Ltd., Dandong, China) and the average diameter of pore-throats in the micromodel was calculated using Eqs. (2)-(4):

$$d_{\text{pore-throat}} = \frac{(d_{\text{pore}} \times \sum l_{\text{pore}}) + (d_{\text{throat}} \times \sum l_{\text{throat}})}{l_{\text{pore-throat}}} \tag{2}$$

$$d_{\text{pore}} = 1.128 a_{\text{pore}} \tag{3}$$

$$d_{\text{throat}} = 1.128 a_{\text{throat}} \tag{4}$$

where d_{pore} is the equivalent diameter of a pore, μm; d_{throat} is the equivalent diameter of a throat, μm; l_{pore} is the length of pores in

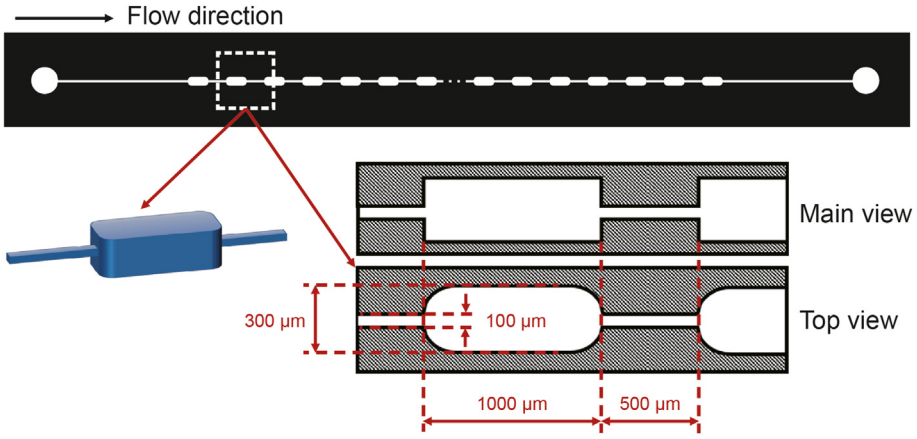

Fig. 1. Schematic diagram of the one-dimensional continuous PTVM.

the micromodel, μm; l_{throat} is the length of throats in the micromodel, μm; a_{pore} is the geometric width of a pore, μm; and a_{throat} is the geometric width of a throat, μm.

2.2.3. Displacement experiment using a two-dimensional heterogeneous PTVM

In order to visually study the influence of matching degree on the profile control performance of EGPs in heterogeneous porous media, a two-dimensional heterogeneous PTVM was designed and fabricated (Mohammadi et al., 2014; Romero-Zeron and Kantzas, 2005). As shown in Fig. 3, a 40 mm × 40 mm chip was manufactured using glass acid etching. The average size of pore-throats could be controlled by the adjusting the etching time. The model consisted of a high-permeability region in the diagonal direction and two low-permeability regions on the upper and lower sides. The average pore-throat diameters in the high permeability and low permeability regions were about 400 μm and 70 μm, respectively.

In the preparation stage of the experiment, the chip was fully saturated with crude oil, and in order to simulate the initial reservoir environment, the saturated chip was aged for 2 weeks at 90°C to ensure that the surface of all pore-throats was lipophilic. Experiments were conducted using the following procedure: (1) Brine water flooding using 0.005 mL/min until oil production was negligible; (2) Injection of EGPs suspension with a specific solid concentration; (3) Subsequent water flooding. Photographic images of remaining oil in the chip were then obtained. The experiment was conducted at 90°C. The oil saturation in the images was estimated using a grayscale recognition method. The binarization method were used to distinguish the oil in the image, and the number of black pixels representing crude oil were counted. The difference in the number of black pixels after different experimental procedure is used to calculate the oil recovery. The above process was realized in Python.

2.2.4. NMR displacement experiment using a three-dimensional heterogeneous core model

Heterogeneous cores are often used to simulate actual porous media of reservoirs (Liu et al., 2019). However, most previous core flooding experiments could only indirectly analyze the migration and retention behavior of particles through pressure curves and explain the mechanisms of EOR by profile control through hypothetical models. With the advancement of technology, the hydrogen signal of crude oil in core flooding can be received and inversed in real time using online NMR technology so as to obtain the flow behavior and profile control mechanism more directly.

A schematic diagram of the online low-field NMR core displacement experimental system (Niumag, LF-NMR, China) is shown in Fig. 4. Fluorine oil, without a nuclear magnetic signal, was used as the medium in the confining pressure system and temperature control system and the core holder was made of non-magnetic material to eliminate noise from the experimental set-up. The NMR displacement experiments using the three-dimensional heterogeneous core were conducted according the following procedures: (1) The heterogeneous core was saturated with crude oil by the pressurized method in a vacuum, created using a vacuum-pressurized saturation device, and the core was saturated with oil and aged at 90°C for two weeks to simulate the environment of an actual reservoir; (2) The NMR base signal was measured using a standard sample; (3) The heterogeneous core was put into the core holder, and an initial T_2 spectra and crude oil distribution image of the heterogeneous core were obtained by NMR scanning and base signal inversion; (4) Non-signalized heavy water was injected to displace the oil until the water-cut reached 98%; (5) 1.0 PV (PV represents pore volume of the high permeability layer) of the EGPs suspension slug, prepared using heavy water, was injected; (6) Subsequent non-signalized heavy water flooding was applied until the water-cut reached 98% again.

Cylindrical heterogeneous cores (100 mm × φ25 mm) were used in the online low-field NMR core displacement experiment. The heterogeneous core was composed of two semi-cylindrical cores with different porosities and permeabilities cemented in the cross section, as shown in Fig. 5. The two semi-cylindrical cores were bonded to form a complete heterogeneous cylindrical core by curing for 24 h in the mold using quartz sand to fill the gap and epoxy resin as cementing agent. The high permeability semi-cylindrical core had a permeability of about 1.1 μm^2 and a porosity of 27%, and the low permeability semi-cylindrical core had a permeability of 0.2 μm^2 and a porosity of 22%. The average pore-throats sizes of the cores were calculated using the Carman-Kozeny equation (Dai et al., 2017).

3. Results and discussion

3.1. Basic physical properties of the EGPs

The prepared EGPs suspension was homogeneous and stable, with a density of about 1.0 g/cm^3, a viscosity of less than 5.0 mPa s and a pH value of about 7. Fig. 6 shows the particle size distributions of typical EGPs suspensions used in this study. It can be seen that the particle size distribution curves exhibit prominent single peaks. This indicates that the particles sizes of the prepared EGPs

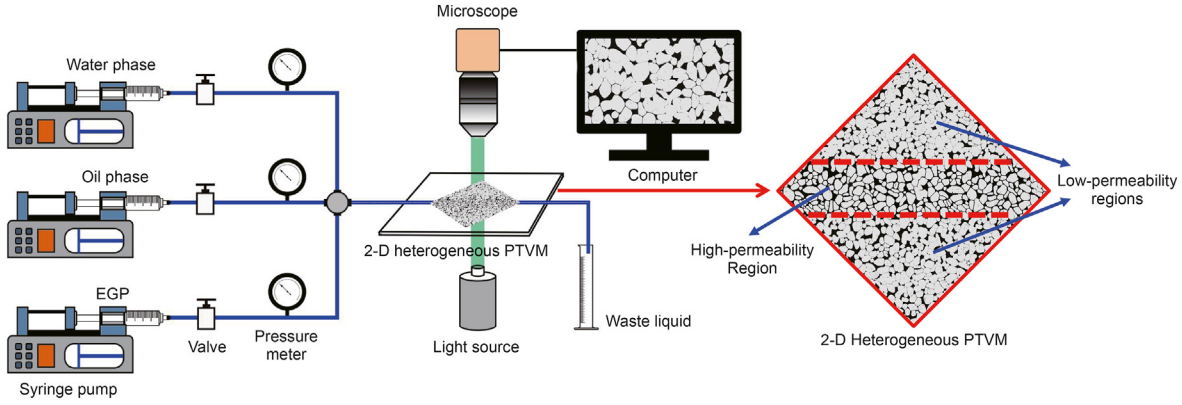

Fig. 3. Schematic diagram of displacement experiment using two-dimensional heterogeneous PTVM.

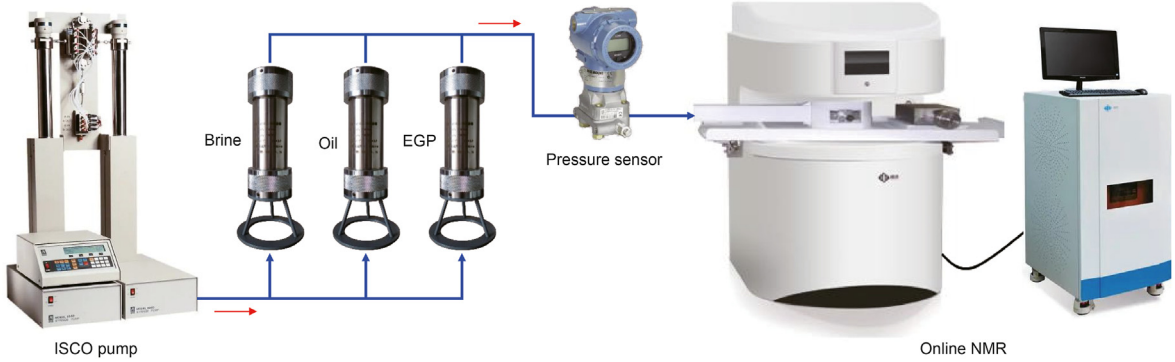

Fig. 4. Schematic diagram of online low-field NMR core displacement experiment.

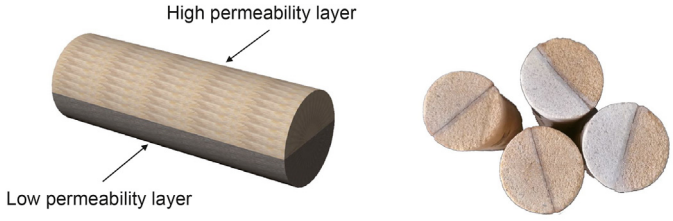

Fig. 5. Images of cylindrical heterogeneous cores.

suspension were relatively uniform. The average particle sizes of the EGPs suspensions prepared using different shearing parameters i.e., 1500 rpm, 1000 rpm and 600 rpm for 5 min, were about 35 μm, 70 μm, and 156 μm, respectively.

Considering that the viscoelasticity of EGPs is difficult to directly measure, its viscoelasticity can be indirectly reflected by measuring the viscoelasticity of the bulk gel (i.e., the raw material used to prepare the EGPs). Fig. 7 shows the storage moduli (G') and loss moduli (G″), measured in the frequency range 0.1 rad/s to 100 rad/s, of the bulk gel used to prepare the EGPs for this study. It can be seen that the storage modulus of the bulk gel was apparently higher than the loss modulus. The high elasticity of the bulk gel means that the prepared particles had high elasticity, which suggests that the EGPs had good deformation-recovery properties and the deformation-recovery characteristics of the EGPs were conducive to its migration and retention in pore-throats.

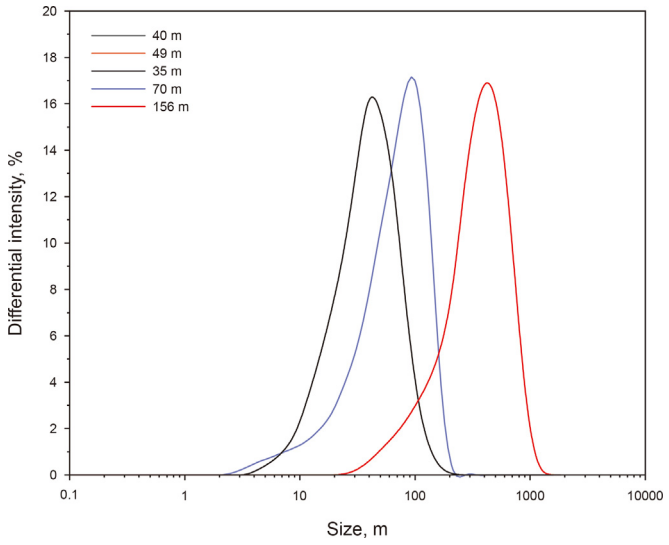

Fig. 6. Particle size distributions of typical EGPs suspensions.

3.2. Migration and retention behaviors of EGPs in the 1-D continuous pore-throat micromodel

During the injection of EGPs suspension and subsequent water flooding, particles migrated and were retained in the continuous pore-throats of the model along the injection direction. In order to obtain the migration and retention characteristics of the EGPs, the final states of particles in each pore-throat after EGPs suspension injection and subsequent water flooding were recorded photographically. The migration and retention behaviors of the EGPs were obviously different due to the different matching coefficients (φ). When the particle size was too small, the EGPs could not form stable retention in the pore-throats, resulting in ineffective plugging. Conversely, when the particle size was oversized, it was difficult for the EGPs to migrate through the pore-throats, resulting in a short effective profile control distance.

To describe this process more fully, we introduce the concept of filling degree (FD), which was obtained by binary processing and image analysis of the pore-throat images, to quantitatively characterize the migration and retention of EGPs at different pore-throat positions. Here FD in a pore is defined as the volume ratio of EGPs to the pore. High value of FD in a pore means that the EGPs could migrate into the pore and form stable retention, which is conducive to effective in-depth profile control of EGPs.

Using this concept, experiments were performed in order to find an optimized value of the matching coefficient. EGPs with different particle sizes were used to study the influence of the matching coefficient on the migration and retention of particles, and the experimental matching coefficient was varied within the range 0.07–0.52.

Experimental results from three matching coefficients are now given in more detail as they typify the range of results obtained:

$$\text{Matching coefficient} = 0.13 \text{ (i.e., } d_{\text{particle}} = 35.3\ \mu\text{m}, d_{\text{pore-throat}} = 253.2\ \mu\text{m}) \quad (1)$$

This was a typical case while the average size of the EGPs was much smaller than that of the pore-throats. After injection of the EGPs suspension and subsequent water flooding, the FD of particles in each pore of the micromodel was recorded and plotted (Fig. 8a). Images of EGPs migration and retention in the head (first pore-throat), middle (eleventh pore-throat) and tail (twenty-first pore-throat) of the micromodel are shown in Fig. 8b and c.

With the small matching coefficient, it can be seen from the

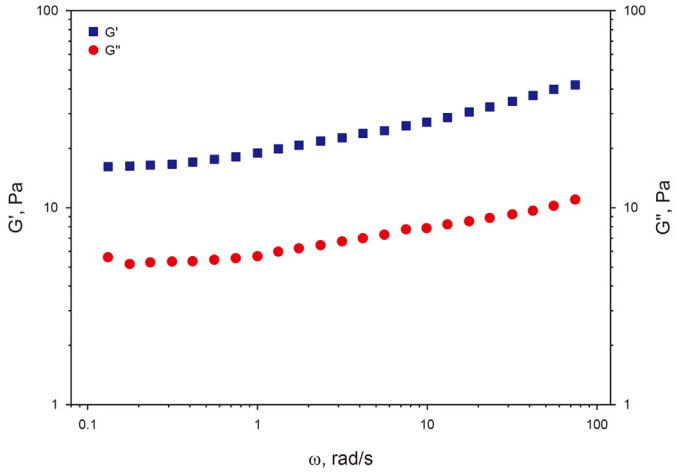

Fig. 7. Storage modulus and loss modulus of the bulk gel used to prepare the EGPs.

results that most of the particles in the injected EGPs suspension directly passed through the pore-throats to enter the more distant pore-throat structures. Only a small number of particles with larger sizes were retained and formed accumulations in the contractions of the pore-throats. Due to the low proportion of larger particles in the EGPs suspension with a small average particle size, the accumulations occurred mostly near the injection point. Moreover, during the subsequent water flooding process, weak accumulations of a small number of particles were destroyed by the deformation and slippage of particles under the action of the injection pressure. Hence most of the particles were washed out of the model by the subsequently injected water, resulting in few particles remaining in pore-throats. The above phenomena can be seen to be detrimental to the profile control performance of EGPs.

$$\text{Matching coefficient} = 0.23 \text{ (i.e., } d_{\text{particle}} = 61.4\ \mu\text{m}, d_{\text{pore-throat}} = 263.2\ \mu\text{m}) \quad (2)$$

This result typified the case for moderate particle sizes. The FD of EGPs in each pore at different stages was recorded and can be seen in Fig. 9a. Images of EGPs migration and retention in the head (first pore-throat), middle (eleventh pore-throat) and tail (twenty-first pore-throat) of the micromodel are shown in Fig. 9b and c.

It can be seen from Fig. 9a that after EGPs suspension injection, all pores of the micromodel were with high FDs. Even after subsequent water flooding, the FDs of all pores remained high. Massive particles still detained in the pores after subsequent water flooding. Only close to the injection head, where there was the most serious erosion by injected water, was there a certain reduction of FD, as shown in Fig. 9b and c. Obviously, under a matching coefficient of 0.23, the particles could smoothly migrate through the depth of the continuous pore-throat model, and could also be retained in the pores stably during the subsequent water flooding process, which is conducive to effective in-depth profile control using EGPs.

$$\text{Matching coefficient} = 0.36 \text{ (i.e., } d_{\text{particle}} = 95.8\ \mu\text{m}, d_{\text{pore-throat}} = 263.2\ \mu\text{m}) \quad (3)$$

This is a typical case of an excessive matching coefficient. The FD of each pore after EGPs suspension injection and subsequent water flooding is presented in Fig. 10a, and images of EGPs migration and retention are shown in Fig. 10b and c.

As can be seen in Fig. 10b, the pore-throat near the injection head was blocked by a single particle, or by the bridging of two particles, as the average diameter of the EGPs was similar to that of the pore-throats. A blockage caused by a single particle, or by the bridging of two particles, was significantly stronger than that caused by the bridging of several particles and made it difficult for particles in the injection head to migrate deeper into the model. As a result, the continuous injection of EGPs caused a sudden increase in injection pressure which exceeded the threshold of the model, resulting in the EGPs injection being terminated. This result indicates that there will be a poor injectivity of EGPs suspension when the matching coefficient is excessive.

It can be seen from Fig. 10c that a few particles with smaller sizes were displaced to deeper pore-throats during the subsequent water flooding process, and the number of particles in the middle and tail side of the model increased slightly. However, the strong blockage at the injection head still prevented most particles from in-depth migration. Fig. 10a shows the FDs of particles in all pores of the model after EGPs injection and subsequent water flooding. It can be seen that although the FDs of the pores near the injection head was high, the pores in the middle and tail part of the model experienced low FDs, which is consistent with the results shown in Fig. 10b and c. In summary, the in-depth migration and injectivity of EGPs is poor under a situation of excessive matching coefficient, which will result in short profile control distances in field applications.

In order to optimize the matching coefficient range, more experiments with different matching coefficients were conducted and the average FD after EGPs injection and the remaining ratio (RR) of EGPs in the pores after subsequent water flooding were recorded. Here RR is defined as the ratio of the residual amount of particles in the pores after subsequent water flooding to the initial amount of particles after EGPs injection, which could reflect the stability of particle accumulation in the continuous pore-throat model against erosion by subsequently injected water.

The results of average FDs and RRs of a series of experimental groups with different matching coefficients are shown in Fig. 11.

It can be seen from Fig. 11 that the results were distributed in three typical regions:

Region I: Here the matching coefficient was smaller than 0.18, and both the average FD and RR of EGPs in the pores were lower than 50%, which indicated that the EGPs could not form enough retention and stable accumulation in the pores.

Region II: When the matching coefficient range was between 0.20 and 0.32, both the FD of pores after EGPs injection and the RR of EGPs after subsequent water flooding were higher than 50%, which indicated that EGPs could migrate and fill most pores during the injection process and form stable accumulations in the pores which could resist erosion by subsequently injected water. Therefore, in the matching coefficient range between 0.20 and 0.32, the EGPs could migrate to the in-depth pore-throats during the injection process and form stable retention in pores during subsequent water flooding, which is conducive to the in-depth profile control of EGPs.

Region III: This region showed that when the matching coefficient was larger than 0.36, although the RR of EGPs after subsequent flooding was high, the FD of pores after EGPs injection was lower than 50%. This indicated that although the oversized EGPs could form stable accumulations and strong blockages in the pore-throats, it was difficult for them to be injected and migrate through the continuous pore-throats. This will result in poor injectability of EGPs in an oilfield application.

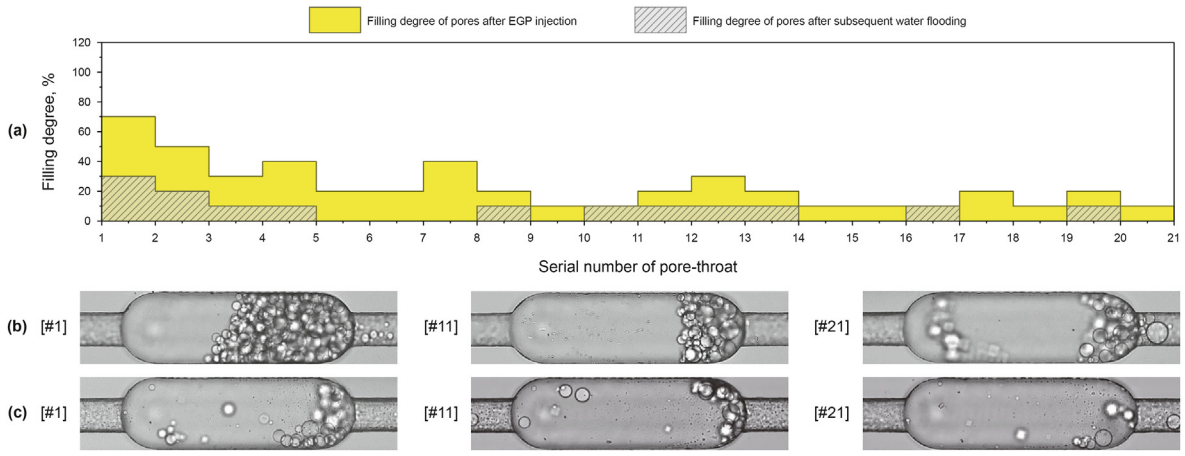

Fig. 8. Filling degrees and images of EGPs in pores with matching coefficient of 0.13: (**a**) filling degree in each pore of the micromodel, (**b**) images of typical pores after EGPs injection, and (**c**) images of typical pores after subsequent water flooding.

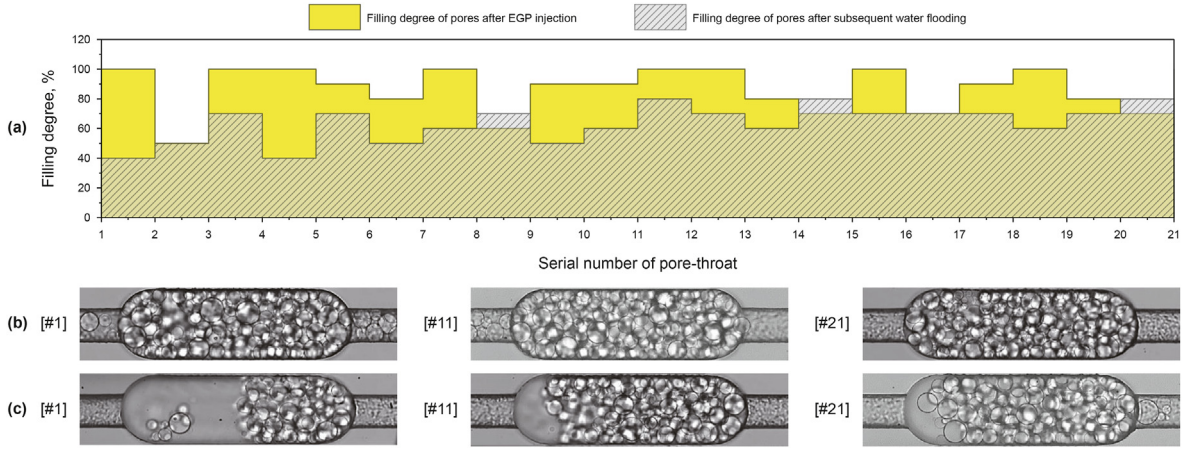

Fig. 9. Filling degrees and images of EGPs in pores with matching coefficient of 0.23: (**a**) filling degree in each pore of the micromodel, (**b**) images of typical pores after EGPs injection, and (**c**) images of typical pores after subsequent water flooding.

3.3. Profile control performance of EGPs in the 2-D heterogeneous pore-throat visualization model

As mentioned above, the matching coefficient directly affects the migration and retention characteristics of EGPs in pore-throats, thereby affecting the profile control effect and determining the final performance of EOR by EGPs. To visually investigate the influence of matching degree on profile control performance of EGPs, a visual simulation experiment using a two-dimensional heterogeneous PTVM was conducted.

The initial water flooding, EGPs suspension injection and subsequent water flooding processes were carried out for three experimental groups with typical matching coefficients, i.e., 0.17, 0.29 and 0.39. The remaining oil distribution within the heterogeneous PTVM after different stages were photographed. Fig. 12a shows the initial oil saturation in the model. Fig. 12b shows the injected water breakthrough along the high-permeability region after initial water flooding, and crude oil in the upper and lower regions with low permeability was not effectively recovered. After injection with EGPs of different matching coefficients followed by subsequent water flooding, the remaining oil distributions in the model are shown in Fig. 12c-e.

It can be seen from Fig. 12c that the remaining oil in the low-permeability regions was swept very little after EGPs injection and subsequent water flooding while the matching coefficient was small ($\varphi = 0.17$), indicating that profile control and EOR performance would be poor. This was because the undersized EGPs was unable to form effective and stable plugging in the pore-throats of the breakthrough channels with high permeability, and the subsequent injection water was hard to be diverted towards the low-permeability regions with high remaining oil saturation. In this case, most of the subsequent injected water still preferred to flow along the high-permeability region, resulting in the oil in the low-permeability regions remaining unswept.

When the matching coefficient was too large ($\varphi = 0.39$), only the remaining oil near the injection end (left part) could be displaced after EGPs injection and subsequent water flooding, and large amounts of oil in the central and outlet parts of the low-permeability regions remained unswept (Fig. 12e). This was because a large number of oversized particles were retained and plugged in the pore-throats of the injection end, and so particles found it difficult to migrate deeply into the high-permeability channels resulting in a

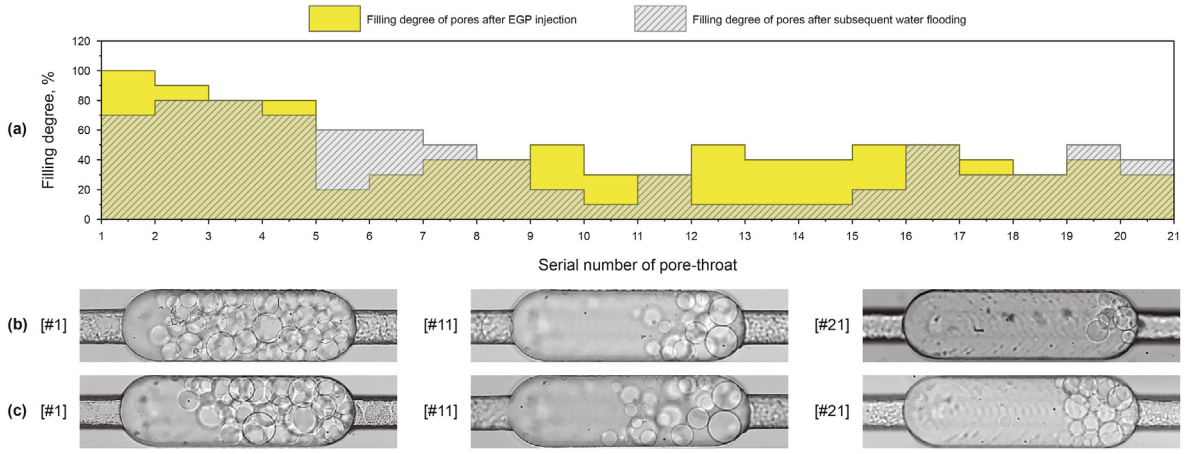

Fig. 10. Filling degrees and images of EGPs in pores with matching coefficient of 0.36: (**a**) filling degree in each pore of the micromodel, (**b**) images of typical pores after EGPs injection, and (**c**) images of typical pores after subsequent water flooding.

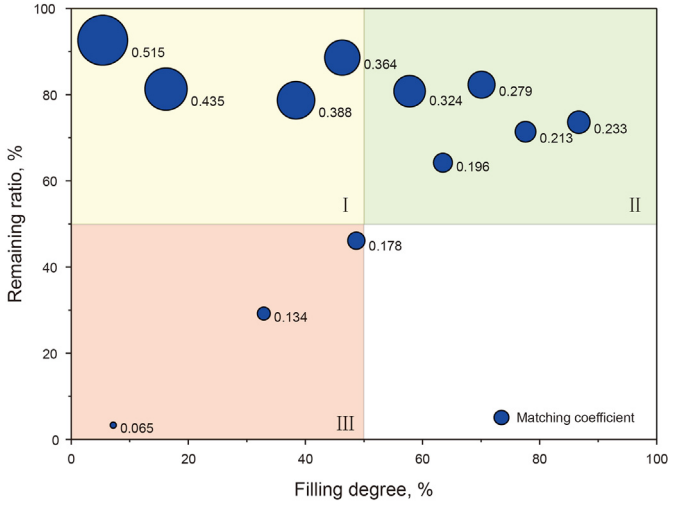

Fig. 11. Filling degree and remaining ratio of EGPs in pores with different matching coefficients.

short distance of profile control. At the beginning of the subsequent water flooding, the injected water was diverted to the low-permeability regions and displaced the remaining oil there as the EGPs caused blockages at the injection end of the high-permeability channels. Nevertheless, as the subsequent water flooding progressed, the injected water flowed back to the high-permeability channels because of the short migration and profile control distance of the EGPs, resulting in the oil in the central and outlet parts of low-permeability regions still remaining unswept.

When the matching coefficient was optimal ($\varphi = 0.29$), most of the remaining oil in the low-permeability regions was swept and displaced after EGPs injection and subsequent water flooding (Fig. 12d). This benefited from the in-depth migration and stable retention of EGPs in the pore-throats of the high-permeability channels, so that the injected water was continuously diverted towards the low-permeability regions to displace the remaining oil during the subsequent water flooding process. Therefore, the profile control and EOR performance was best for this case.

In order to quantitatively analyze the influence of the matching coefficient on the performance of profile control and EOR by EGPs, the black pixels representing residual oil were extracted from the collected images and the proportions of remaining oil in different regions were estimated, using image processing, after final subsequent water flooding. The results are presented in Table 2.

It can be seen that the proportion of remaining oil was highest when the matching coefficient was small. In this case more than 55% of the crude oil in the low-permeability regions could not be displaced even after the final subsequent water flooding. When the matching coefficient was too large, although the oil recovery slightly increased compared with the case of small matching coefficient, there was still about 40% of the crude oil left in the low-permeability regions. When the experiment was conducted with an optimal matching coefficient, most of the crude oil in the model was displaced out, and the remaining oil in the low-permeability regions decreased to less than 20% with only a few marginal areas being unswept after subsequent water flooding.

Based on the above discussion it can be seen that the matching relationship between EGPs and pore-throats plays a key role in the performance of profile control and EOR. The final oil recovery from low-permeability regions in the heterogeneous pore-throat model could be increased by more than 35% due to the in-depth migration and stable retention of EGPs in pore-throats under an optimal matching coefficient condition.

3.4. Profile control performance of EGPs in the 3-D heterogeneous core model

Displacement experiments using 3-D heterogeneous cores were carried out to investigate the profile control characteristics of EGPs in actual reservoir porous media. Three typical matching coefficient experimental groups were used to analyze the influence of the matching degree between EGPs and pore-throats on oil displacement efficiency within oil layers with different permeabilities using an online low-field NMR core displacement experimental system. Distribution images and T_2 spectra of crude oil after initial saturation by crude oil, initial water flooding, EGPs suspension injection and subsequent water flooding were obtained.

Fig. 13(I) shows the saturation distribution images of crude oil in core after different process stages for the case while the matching coefficient was small ($\varphi = 0.14$). It can be seen that after initial oil saturation, both the high-permeability layer and low-permeability

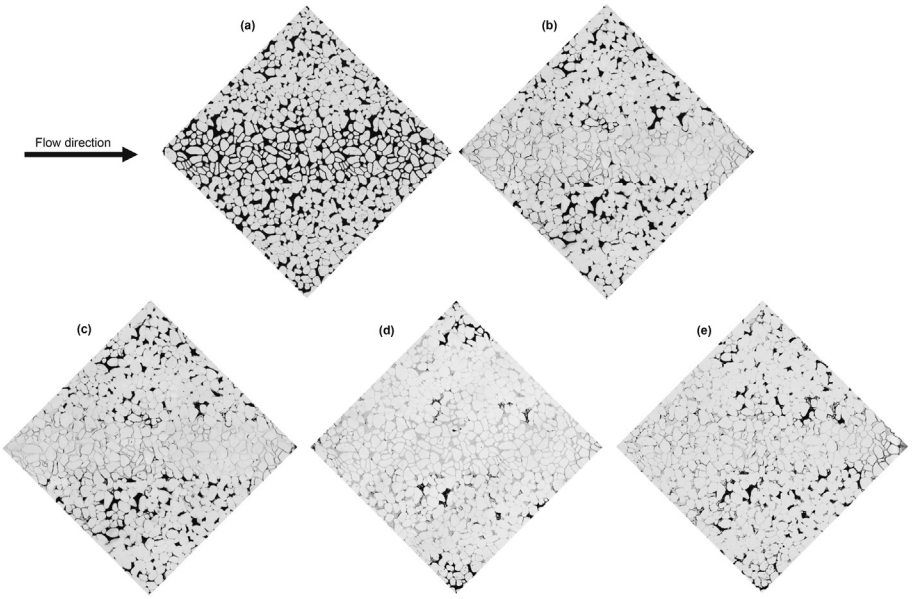

Fig. 12. Images of remaining oil distribution within the heterogeneous PTVM after different stages: (**a**) original state after initial oil saturation, (**b**) after initial water flooding, (**c**) final state for the case with $\varphi = 0.17$, (**d**) final state for the case with $\varphi = 0.29$, and (**e**) final state for the case with $\varphi = 0.39$.

Table 2
Proportions of remaining oil in different regions after final subsequent water flooding.

Residual	Region	Region	Region
	Low permeability zone (Upper)	High permeability zone	Low permeability zone (Lower)
$\varphi = 0.17$	55.14%	12.40%	59.06%
$\varphi = 0.29$	14.08%	2.59%	21.05%
$\varphi = 0.39$	37.56%	11.57%	41.40%

layer had high oil saturation (Fig. 13(I)a). After initial water flooding, the oil saturation in the high-permeability layer significantly reduced (Fig. 13(I)b). Meanwhile, an obvious water breakthrough channel was formed in the high-permeability layer, resulting in oil in other regions not being swept, which was consistent with the development process of most water-flooded reservoirs. It can be seen from Fig. 13(I)c that the injection of EGPs had little effect on the oil saturation in the core. With the subsequent water flooding, only a small amount of oil in the high-permeability layer was displaced due to the weak flow control effect of the injected EGPs. However, the remaining oil in the low-permeability layer was not well swept (Fig. 13(I)d). These results indicate that the EGPs could not form effective plugging in the high-permeability layer when there was a small matching coefficient, which led to poor profile control performance and failure of water diversion to the low-permeability layer with high remaining oil saturation.

Fig. 13 (III) shows the results when the matching coefficient was large ($\varphi = 0.39$). As can be seen in Fig. 13 (III)a and Fig. 13 (III)b, the NMR images of crude oil in the heterogeneous core after initial oil saturation and initial water flooding were similar to those for the small matching coefficient (Fig. 13I). A water breakthrough channel was formed in the high-permeability layer, and oil in the low-permeability layer was barely displaced by injected water. However, the oil recovery after EGPs injection and subsequent water flooding was slightly better than the case with the small matching coefficient. It can be seen from Fig. 13 (III)c and Fig. 13(III)d that some oil in the front half of the low-permeability layer was displaced after EGPs injection and subsequent water flooding, while the oil in the rear half remained unswept. This result was because the oversized EGPs could not migrate through the pore-throats, resulting in strong plugging near the injection end and a short profile control distance. Although the injected water was diverted to the low-permeability layer to displace the remaining oil due to the plugging by EGPs in the high-permeability layer in the early period of the subsequent water flooding, the injected water flow returned to the formed water breakthrough channel after exceeding the limited migration distance of the EGPs, which led to poor recovery of oil in the rear half of the low-permeability layer.

Fig. 13(II) shows the saturation distributions of crude oil for the case with a moderate matching coefficient ($\varphi = 0.26$). The saturation distributions of crude oil were similar to the above two cases after initial oil saturation and initial water flooding (Fig. 13(II)a and Fig. 13(II)b). However, it is obvious that the remaining oil in the core was almost displaced after EGPs injection and subsequent water flooding, and only a small amount of residual oil could not be recovered (Fig. 13(II)c and Fig. 13(II)d). This excellent result benefited from the effective in-depth profile control performance of EGPs which was contributed to the deep migration and stable retention of particles with suitable sizes. The subsequently injected water mainly flowed through the low-permeability layer due to the effective in-depth profile control of the EGPs, resulting in the highest potential for efficient EOR.

In order to quantitatively describe the oil recoveries from the high and low permeability layers in the three-dimensional

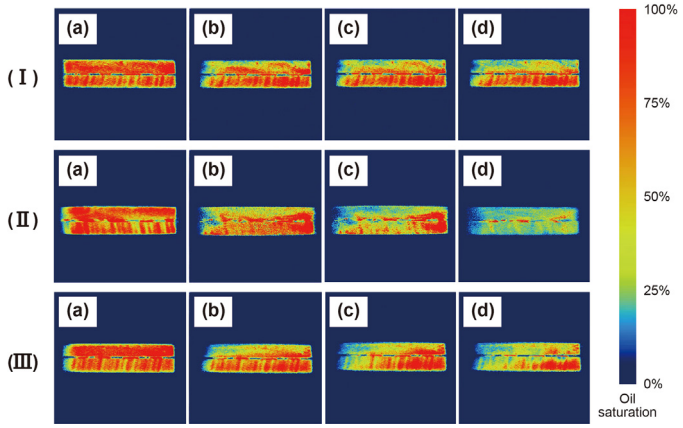

Fig. 13. Saturation distribution images of crude oil in core after different stages: (I) for the case with $\varphi = 0.14$, (II) for the case with $\varphi = 0.26$, (III) for the case with $\varphi = 0.39$, (**a**) after initial oil saturation, (**b**) after initial water flooding, (**c**) after EGPs injection, and (**d**) after subsequent water flooding.

heterogeneous porous media under different matching coefficients, the T_2 spectra at different stages within the above three experimental groups were analyzed (Fig. 14). According to the NMR theorem, different relaxation time reflects different quantities of crude oil in pores with different sizes, and the integral area represents the amount of accumulated crude oil. It can be seen from the T_2 spectrum curves and integral areas that when the matching coefficient was small, only oil in high-permeability layer was recovered markedly in the whole displacement process. The oil recovery in the low-permeability layer could only be slightly improved with an EOR of 12.4% by EGPs injection and subsequent water flooding processes due to the poor profile control performance of EGPs for this case (Fig. 14a and d). When the matching coefficient was too large, part of the crude oil in the small-sized pores of the low-permeability layer was recovered, and the EOR for the low-permeability layer by EGPs injection and subsequent water flooding processes was 22.4% (Fig. 14c and d). Although the EOR in this case was better than that for the case with a small matching coefficient, it was not the highest due to the short profile control distance of the EGPs. In the case of a moderate matching coefficient, due to the in-depth profile control effect of the EGPs,

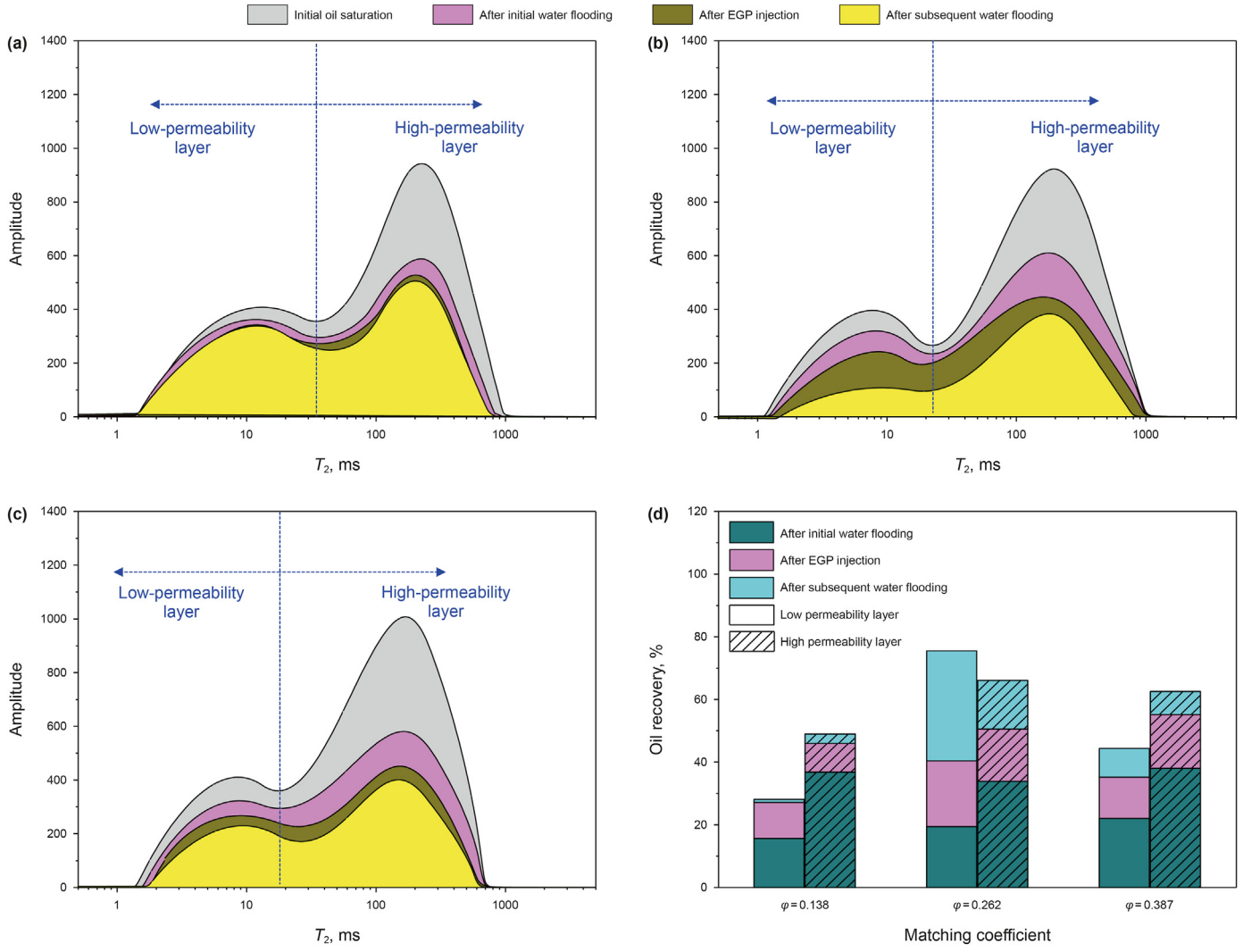

Fig. 14. T_2 spectrum curves and oil recoveries after different stages: (**a**) T_2 spectrum curves for the case with $\varphi = 0.14$, (**b**) T_2 spectrum curves for the case with $\varphi = 0.26$, (**c**) T_2 spectrum curves for the case with $\varphi = 0.39$, and (**d**) oil recoveries of the high- and low-permeability layer.

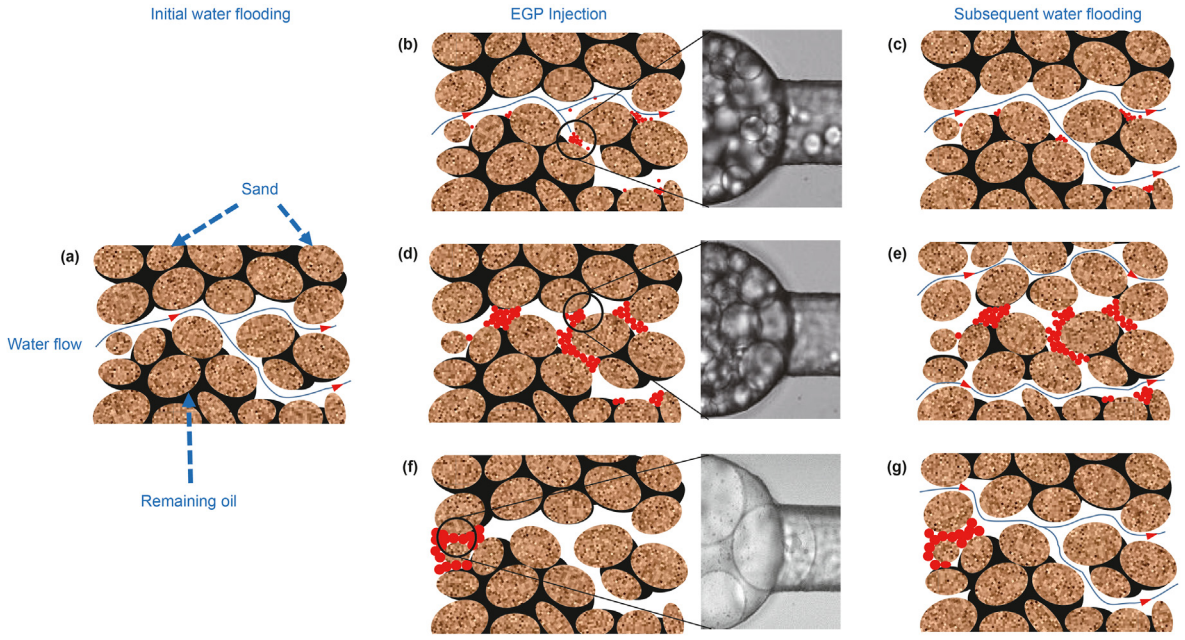

Fig. 15. Schematic illustration of migration and retention mechanism influencing profile control of EGPs: (**a**) water breakthrough channels formed in high-permeability regions, (**b**) migration and retention of EGPs with a small φ, (**c**) breakthrough flow of subsequent injected water with a small φ, (**d**) migration and retention of EGPs with an optimal φ, (**e**) fluid diversion of subsequent injected water with an optimal φ, (**f**) migration and retention of EGPs with an excessive φ, and (**g**) detour flow of subsequent injected water with an excessive φ.

most of the crude oil in the small-sized pores of the low-permeability layer was recovered (Fig. 14b and d). In this case, the EOR for the low-permeability layer was the highest (56.1%) by EGPs injection and subsequent water flooding.

3.5. Migration and retention mechanism influencing profile control of EGPs

Based on the above results, the mechanism which influences the migration and retention characteristics of the profile control of EGPs is summarized in Fig. 15. A water breakthrough channel is formed in high-permeability regions during long-term water flooding, resulting in ineffective flooding of injected water and leaving large amounts of oil unswept in low-permeability regions (Fig. 15a). The above phenomenon is a common problem faced by water flooding development in oilfields. Profile control treatment by EGPs is frequently applied to improve water flooding efficiency. However, significant differences exist in the performance by EGPs due to the differences in particle migration and retention characteristics influenced by the matching coefficient.

As shown in Fig. 15b, if the matching coefficient is too small ($\varphi < 0.20$), although undersized EGPs can migrate deeply through the pore-throats, it is difficult to form stable retention in the pores. The subsequently injected water will wash away the particles making profile control ineffective. The injected water is then not diverted to low-permeability regions with high remaining oil saturation, resulting in poor EOR by EGPs injection (Fig. 15c).

If the matching coefficient is too large ($\varphi > 0.32$), although the oversized EGPs can form blockages in the high-permeability water breakthrough channel near the injection end (Fig. 15f), the particles find it difficult to migrate to the in-depth pore-throats, resulting in a short profile control distance. During the subsequent water flooding process, the injected water detours back to the water breakthrough channel due to the short profile control distance, which leads to only a small amount of remaining oil in low-permeability regions being swept (Fig. 15g). The EOR by EGPs injection is not high in this case.

As shown in Fig. 15d, only if the matching coefficient is within the optimized range ($0.20 \leq \varphi \leq 0.32$), can the EGPs with moderate sizes migrate deeply and form stable retention in the pore-throats of water breakthrough channels in high-permeability regions. The subsequently injected water is diverted to low-permeability regions to displace the remaining oil due to the effective plugging by the EGPs of the high-permeability water breakthrough channels, which contributes to the excellent performance of EOR by EGPs injection, as shown in Fig. 15e.

4. Conclusions

In this work, the pore-scale migration, retention and controlling mechanism of migration and retention characteristics on EOR by profile control using EGPs were investigated. The matching coefficient was used to investigate its influence on migration, retention and profile control performance of EGPs. A 1-D continuous PTVM, a 2-D heterogeneous PTVM and a 3-D heterogeneous core model were constructed and used to elucidated the migration and retention characteristics of EGPs in pore-throats, identified the mechanisms of migration and retention, and examined their influence on EOR by EGPs profile control. The major conclusions are summarized as follows:

(1) While the matching coefficient was in the optimal range (i.e., 0.20–0.32), the EGPs could not only smoothly migrate to the deeper pore-throats, but also form stable retention in the pores to resist the erosion of injected water, which was

conducive to the effective in-depth profile control by the EGPs.

(2) Marked differences existed between EOR performances using EGPs profile control with different matching coefficients. The EOR with an optimal matching coefficient was much higher than that in cases with a smaller matching coefficient or an excessive matching coefficient. The EOR in the low-permeability layer of 3-D heterogeneous core model were 12.4%, 56.1% and 22.4% with matching coefficients of 0.14, 0.26 and 0.39, respectively.

(3) The sweep efficiency in low-permeability regions could be significantly improved by in-depth migration and stable retention of EGPs in the pore-throats with an optimal matching coefficient, which was much better than that in cases with a smaller matching coefficient or an excessive matching coefficient.

(4) If the matching coefficient is too small, the subsequently injected water will wash away the particles along the water breakthrough channels due to unstable retention of EGPs in the pores, making profile control ineffective.

(5) If the matching coefficient is too large, the subsequently injected water detours back to the water breakthrough channels due to poor deep migration ability of EGPs in the pore-throats, making profile control distance short.

Acknowledgments

The work was supported by the National Key Research and Development Project (2019YFA0708700), the National Natural Science Foundation of China (52104061), the project funded by China Postdoctoral Science Foundation (2020M682264), the Shandong Provincial Natural Science Foundation (ZR2021QE075) and the Fundamental Research Funds for the Central Universities (20CX06090A). The authors express their appreciation to technical reviewers for their constructive comments.

References

Bai, B.J., Liu, Y.Z., Coste, J.P., Li, L.X., 2007. Preformed particle gel for conformance control: transport mechanism through porous media. SPE Reservoir Eval. Eng. 10, 176–184. https://doi.org/10.2118/89468-PA.

Cui, G.D., Ning, F.L., Dou, B., Li, T., Zhou, Q.C., 2021. Particle migration and formation damage during geothermal exploitation from weakly consolidated sandstone reservoirs via water and CO2 recycling. Energy, 122507. https://doi.org/10.1016/j.energy.2021.122507.

Dai, C.L., Liu, Y.F., Zou, C.W., You, Q., Yang, S., Zhao, M.W., Zhao, G., Wu, Y.N., Sun, Y.P., 2017. Investigation on matching relationship between dispersed particle gel (DPG) and reservoir pore-throats for in-depth profile control. Fuel 207, 109–120. https://doi.org/10.1016/j.fuel.2017.06.076.

Dai, C.L., Zou, C.W., Liu, Y.F., You, Q., Tong, Y., Wu, C., Shan, C.H., 2018. Matching principle and in-depth profile control mechanism between elastic dispersed particle gel and pore throat. Acta Petrol. Sin. 39 (4), 427–434. https://doi.org/10.7623/syxb201804006 (in Chinese).

Elsharafi, M.O., Bai, B.J., 2017. Experimental work to determine the effect of load pressure on the gel pack permeability of strong and weak preformed particle gels. Fuel 188, 332–342. https://doi.org/10.1016/j.fuel.2016.10.001.

Feng, Q.H., Cha, L.M., Dai, C.L., Zhao, G., Wang, S., 2020. Effect of particle size and concentration on the migration behavior in porous media by coupling computational fluid dynamics and discrete element method. Powder Technol. 360, 704–714. https://doi.org/10.1016/j.powtec.2019.10.011.

Goudarzi, A., Zhang, H., Varavei, A., Hu, Y.P., Delshad, M., Bai, B.J., Sepehrnoori, K., 2013. Water management in mature oil fields using preformed particle gels. In: SPE Western Regional & AAPG Pacific Section Meeting 2013 Joint Technical Conference, 19-25 April, Monterey, California, USA. https://doi.org/10.2118/165356-MS.

Imqam, A., Bai, B.J., Ramadan, M.A., Wei, M.Z., Delshad, M., Sepehrnoori, K., 2015. Preformed-particle-gel extrusion through open conduits during conformance-control treatments. SPE J. 20 (5), 1083–1093. https://doi.org/10.2118/169107-PA.

Imqam, A., Wang, Z., Bai, B.J., 2017. Preformed-particle-gel transport through heterogeneous void-space conduits. SPE J. 22 (5), 1437–1447. https://doi.org/10.2118/179705-PA.

Jia, H., Pu, W.F., Zhao, J.Z., Jin, F.Y., 2010. Research on the gelation performance of low toxic PEI cross-linking PHPAM gel systems as water shutoff agents in low temperature reservoirs. Ind. Eng. Chem. Res. 49 (20), 9618–9624. https://doi.org/10.1021/ie100888q.

Kabir, A.H., 2001. Chemical water & gas shutoff technology - an overview. In: SPE Asia Pacific Improved Oil Recovery Conference, 8-9 October, Kuala Lumpur, Malaysia. https://doi.org/10.2118/72119-MS.

Lei, G., Gu, S.H., Dong, L.F., Liao, Q.Z., Xue, L., 2021. Particle plugging in porous media under stress dependence by Monte Carlo simulations. J. Petrol. Sci. Eng. 207, 109144. https://doi.org/10.1016/j.petrol.2021.109144.

Liu, X.E., 1995. Development and application of the water control and profile modification technology in China oil fields. In: International Meeting on Petroleum Engineering, 14-17 November, Beijing, China. https://doi.org/10.2118/29907-MS.

Liu, Y.Z., Bai, B.J., Wang, Y.F., 2010. Applied technologies and prospects of conformance control treatments in China. Oil Gas Sci. Technol. 65 (6), 859–878. https://doi.org/10.2516/ogst/2009057.

Liu, Y.F., Dai, C.L., Wang, K., Zhao, M.W., Gao, M.W., Yang, Z., Fang, J.C., Wu, Y.N., 2016. Investigation on preparation and profile control mechanisms of the dispersed particle gels (DPG) formed from phenol–formaldehyde cross-linked polymer gel. Ind. Eng. Chem. Res. 55 (22), 6284–6292. https://doi.org/10.1021/acs.iecr.6b00055.

Liu, Y.F., Dai, C.L., Wang, K., Zou, C.W., Gao, M.W., Fang, Y.C., Zhao, M.W., Wu, Y.N., You, Q., 2017. Study on a novel cross-linked polymer gel strengthened with silica nanoparticles. Energy Fuel. 31 (9), 9152–9161. https://doi.org/10.1021/acs.energyfuels.7b01432.

Liu, Y.F., Zou, C.W., Zhou, D.Y., Li, H., Gao, M.W., Zhao, G., Dai, C.L., 2019. Novel chemical flooding system based on dispersed particle gel coupling in-depth profile control and high efficient oil displacement. Energy Fuel. 33 (4), 3123–3132. https://doi.org/10.1021/acs.energyfuels.9b00243.

Long, Y.F., Yu, B.W., Zhu, C.Q., 2018. Conformance improvement for ultra-high-temperature reservoir: a comparative study between hydrostable and conventional preformed particle gel. In: Abu Dhabi International Petroleum Exhibition & Conference, 12-15 November, Abu Dhabi, UAE. https://doi.org/10.2118/192738-MS.

Mohammadi, S., Kharrat, R., Masihi, M., Ghazanfari, M.H., Saidian, M., 2014. Monitoring the effect of discontinuous shales on the surfactant flooding performance in heavy oil reservoirs using 2D glass micromodels. Petrol. Sci. Technol. 32 (12), 1404–1417. https://doi.org/10.1080/10916466.2010.531351.

Ren, C.F., Li, J.J., Li, Y.Q., Yuan, J.S., Xi, Y.Q., Xiao, K., Wang, Y.X., 2016. Experimental investigation of the matching relationship between asphalt particle and reservoir pore in profile control process. Adv. Mater. Sci. Eng., 2507316 https://doi.org/10.1155/2016/2507316, 2016.

Romero-Zeron, L., Kantzas, A., 2005. Pore-scale visualization of foamed gel propagation and trapping in a pore network micromodel. J. Can. Petrol. Technol. 44 (5), 44–50. https://doi.org/10.2118/05-05-03.

Sang, Q., Li, Y.J., Yu, L., Li, Z.Q., Dong, M.Z., 2014. Enhanced oil recovery by branched-preformed particle gel injection in parallel-sandpack models. Fuel 136, 295–306. https://doi.org/10.1016/j.fuel.2014.07.065.

Tang, X.C., Yang, H.B., Gao, Y.B., Lashari, Z.A., Cao, C.X., Kang, W.L., 2018. Preparation of a micron-size silica-reinforced polymer microsphere and evaluation of its properties as a plugging agent. Colloid. Surface. 547, 8–18. https://doi.org/10.1016/j.colsurfa.2018.03.034.

Wang, C.S., Sun, Z.X., Sun, Q.J., Zhang, L., Zhang, X.Q., 2021. Comprehensive evaluation of waterflooding front in low-permeability reservoir. Energy Sci. Eng. 9 (9), 1394–1408. https://doi.org/10.1002/ese3.948.

Wang, D.M., Han, P.H., Shao, Z.B., Hou, W.H., Seright, R.S., 2008. Sweep-improvement options for the Daqing oil field. SPE Reservoir Eval. Eng. 11 (1), 18–26. https://doi.org/10.2118/99441-PA.

Wu, Y.S., Bai, B.J., 2008. Modeling particle gel propagation in porous media. In: SPE Annual Technical Conference and Exhibition, 21-24 September, Denver, Colorado, USA. https://doi.org/10.2118/115678-MS.

Wu, Y.N., Fang, S.S., Dai, C.L., Sun, Y.P., Fang, J.C., Liu, Y.F., He, L., 2017. Investigation on bubble snap-off in 3-D pore-throat micro-structures. J. Ind. Eng. Chem. 54, 69–74. https://doi.org/10.1016/j.jiec.2017.05.019.

Yang, H.B., Kang, W.L., Yin, X., Tang, X.C., Song, S.Y., Lashari, Z.A., Bai, B.J., Sarsenbekuly, B., 2017. Research on matching mechanism between polymer microspheres with different storage modulus and pore throats in the reservoir. Powder Technol. 313, 191–200. https://doi.org/10.1016/j.powtec.2017.03.023.

Yao, C.J., Lei, G.L., Cathles, L.M., Steenhuis, T.S., 2014. Pore-scale investigation of micron-size polyacrylamide elastic microspheres (MPEMs) transport and retention in saturated porous media. Environ. Sci. Technol. 48 (9), 5329–5335. https://doi.org/10.1021/es500077s.

Yao, C.J., Lei, G.L., Hou, J., Xu, X.H., Wang, D., Steenhuis, T.S., 2015. Enhanced oil recovery using micron-size polyacrylamide elastic microspheres: underlying mechanisms and displacement experiments. Ind. Eng. Chem. Res. 54 (43), 10925–10934. https://doi.org/10.1021/acs.iecr.5b02717.

Yao, C.J., Lei, G.L., Li, L., Gao, X.M., 2012. Selectivity of pore-scale elastic microspheres as a novel profile control and oil displacement agent. Energy Fuel. 26 (8),

5092–5101. https://doi.org/10.1021/ef300689c.
You, Q., Tang, Y.C., Dai, C.L., Zhao, M.W., Zhao, F.L., 2014. A study on the morphology of a dispersed particle gel used as a profile control agent for improved oil recovery. J. Chem. Neuroanat. https://doi.org/10.1155/2014/150256, 2014.
You, Q., Wen, Q.Y., Fang, J.C., Guo, M., Zhang, Q.S., Dai, C.L., 2019. Experimental study on lateral flooding for enhanced oil recovery in bottom-water reservoir with high water cut. J. Petrol. Sci. Eng. 174, 747–756. https://doi.org/10.1016/j.petrol.2018.11.053.
Zhang, G.Y., Seright, R.S., 2007. Conformance and mobility control: foams versus polymers. In: International Symposium on Oilfield Chemistry, 28 February-2 March, Houston, Texas, USA. https://doi.org/10.2118/105907-MS.
Zhao, Y., Bai, B.J., 2022. Selective penetration behavior of microgels in super-permeable channels and reservoir matrices. J. Petrol. Sci. Eng. 210, 109897. https://doi.org/10.1016/j.petrol.2021.109897.
Zhou, X., Wang, Y.C., Zhang, L.H., Zhang, K.W., Jiang, Q., Pu, H.B., Wang, L., Yuan, Q.W., 2020. Evaluation of enhanced oil recovery potential using gas/water flooding in a tight oil reservoir. Fuel 272, 117706. https://doi.org/10.1016/j.fuel.2020.117706.
Zhu, W.Y., Ma, Q.P., Han, H.Y., 2021. Theoretical study on profile control of a nano-microparticle dispersion system based on fracture-matrix dual media by a low-permeability reservoir. Energy Rep. 7, 1488–1500. https://doi.org/10.1016/j.egyr.2021.01.089.